Calculated Hydride Donor Abilities of Five-Coordinate Transition Metal Hydrides $[HM(diphosphine)_2]^+$ (M = Ni, Pd, Pt) as a Function of the Bite Angle and Twist Angle of Diphosphine Ligands

Mark R. Nimlos,*[,†] Christopher H. Chang,[†] Calvin J. Curtis,[†] Alex Miedaner,[†] Heidi M. Pilath,[†] and Daniel L. DuBois[‡]

National Renewable Energy Laboratory, Golden, Colorado 80401, and Pacific Northwest National Laboratory, 902 Battelle Boulevard, Richland, Washington 99352

Received December 4, 2007

Density functional theory (BLYP and B3LYP) and the polarized continuum model (PCM-UA0) for solvation have been used to investigate the effect of bite angle (P−M−P) of diphosphine ligands and the dihedral or twist angle between diphosphine ligands on the hydride donor abilities of Ni, Pd, and Pt $[HM(diphosphine)_2]^+$ complexes. It is found that an increased bite angle for a given transition metal atom results in poorer hydride donor abilities. However, hydride donor abilities for these complexes also decrease as the size of the alkyl side groups on the phosphorus atom increase (Et > Me > H) and with the length of the metal phosphorus bond (Ni > Pd ≅ Pt). These trends correlate with an increase in the twist angle between the two diphosphine ligands, which increases from 0° for a square-planar configuration to 90° for a tetrahedral geometry. Shorter M−P bonds, larger substituents on the diphosphine ligands, and larger bite angles all result in increased steric interactions between diphosphine ligands and larger dihedral or twist angles between the diphosphine ligands. The twist angle correlates much more strongly with hydride donor abilities than do bite angles alone. As the twist angle increases, the hydride donor ability decreases in a linear fashion. A frontier orbital analysis has been carried out, and it is shown that the hydride donor ability of $[HM(diphosphine)_2]^+$ complexes is largely determined by the energy of the lowest unoccupied molecular orbital of the corresponding $[M(diphosphine)_2]^{2+}$ complex.

Introduction

Hydride donor/acceptor abilities of transition metal complexes are an important fundamental quantity for many catalytic processes. For example, the oxidation of H_2 by hydrogenase enzymes and some synthetic catalysts is thought to involve the heterolytic cleavage of H_2 in which a metal atom of the active site serves as a hydride acceptor. In the reverse process, H_2 production, the metal serves as a hydride donor.[1–5] Similarly, ionic hydrogenations are thought to occur by a proton transfer followed by a hydride transfer.[6–9] The abilities of various classes of compounds to function as hydride donors have been based on both kinetic and thermodynamic studies.[6,10–28] In the present work the thermodynamic hydride donor ability is determined

* Corresponding author. E-mail: mark_nimlos@nrel.gov.
† National Renewable Energy Laboratory.
‡ Pacific Northwest National Laboratory.

(1) Nicolet, Y.; de Lacey, A. L.; Vernede, X.; Fernandez, V. M.; Hatchikian, E. C.; Fontecilla-Camps, J. C. Crystallographic and FTIR spectroscopic evidence of changes in Fe coordination upon reduction of the active site of the Fe-only hydrogenase from *Desulfovibrio desulfuricans*. *J. Am. Chem. Soc.* **2001**, *123* (8), 1596–1601.

(2) Peters, J. W.; Lanzilotta, W. N.; Lemon, B. J.; Seefeldt, L. C. X-ray crystal structure of the Fe-only hydrogenase (Cpl) from *Clostridium pasteurianum* to 1.8 Å resolution. *Science* **1998**, *282* (5395), 1853–1858.

(3) Pereira, A. S.; Tavares, P.; Moura, I.; Moura, J. J. G.; Huynh, B. H. Mossbauer characterization of the iron-sulfur clusters in *Desulfovibrio vulgaris* hydrogenase. *J. Am. Chem. Soc.* **2001**, *123* (12), 2771–2782.

(4) Higuchi, Y.; Ogata, H.; Miki, K.; Yasuoka, N.; Yagi, T. Removal of the bridging ligand atom at the Ni-Fe active site of [NiFe] hydrogenase upon reduction with H^{-2}, as revealed by X-ray structure analysis at 1.4 Å resolution. *Structure* **1999**, *7* (5), 549–556.

(5) Volbeda, A.; Fontecilla-Camps, J. C. The active site and catalytic mechanism of NiFe hydrogenases. *Dalton Trans.* **2003**, (21), 4030–4038.

(6) Gaus, P. L.; Kao, S. C.; Youngdahl, K.; Darensbourg, M. Y. Anionic Group-6 Transition-Metal Carbonyl Hydrides As Reducing Agents - Ketones, Aldehydes, and Epoxides. *J. Am. Chem. Soc.* **1985**, *107* (8), 2428–2434.

(7) Gibson, D. H.; Elomrani, Y. S. Selective Reductions of Carbonyl-Compounds with Group 6 Metal-Carbonyl Hydrides. *Organometallics* **1985**, *4* (8), 1473–1475.

(8) Bullock, R. M.; Song, J. S. Ionic Hydrogenations of Hindered Olefins at Low-Temperature−Hydride-Transfer Reactions of Transition-Metal Hydrides. *J. Am. Chem. Soc.* **1994**, *116* (19), 8602–8612.

(9) Magee, M. P.; Norton, J. R. Stoichiometric, Catalytic, and Enantioface-Selective Hydrogenation of C=N Bonds by an Ionic Mechanism. *J. Am. Chem. Soc.* **2001**, *123* (8), 1778–1779.

(10) Cheng, J. P.; Lu, Y.; Zhu, X. Q.; Mu, L. J. Energetics of Multistep versus One-Step Hydride Transfer Reactions of Reduced Nicotinamide Adenine Dinucleotide (NADH) Models with Organic Cations and *p*-Quinones. *J. Org. Chem.* **1998**, *63* (18), 6108–6114.

(11) Anne, A.; Moiroux, J. Redox Potentials and Acid−Base Equilibria of NADH/NAD^+ Analogs in Acetonitrile. *J. Org. Chem.* **1990**, *55* (15), 4608–4614.

(12) Klippenstein, J.; Arya, P.; Wayner, D. D. M. Relative Bond-Dissociation Energies for Some NADH Model Compounds from Hydride Transfer Electron-Transfer Equilibria in Acetonitrile. *J. Org. Chem.* **1991**, *56* (24), 6736–6737.

(13) Kreevoy, M. M.; Ostovic, D.; Lee, I. S. H.; Binder, D. A.; King, G. W. Structure Sensitivity of the Marcus-Lambda for Hydride Transfer between NAD^+ Analogs. *J. Am. Chem. Soc.* **1988**, *110* (2), 524–530.

(14) Sarker, N.; Bruno, J. W. Thermodynamic and kinetic studies of hydride transfer for a series of molybdenum and tungsten hydrides. *J. Am. Chem. Soc.* **1999**, *121* (10), 2174–2180.

(15) Labinger, J. A.; Komadina, K. H. Hydridic Character of Early Transition-Metal Hydride Complexes. *J. Organomet. Chem.* **1978**, *155* (2), C25−C28.

(16) Kao, S. C.; Spillett, C. T.; Ash, C.; Lusk, R.; Park, Y. K.; Darensbourg, M. Y. Relative Reactivity and Mechanistic Studies of the Hydride-Transfer Reagents $HM(CO)_4L^-$ (M = Cr, W – *L* = CO, PR_3). *Organometallics* **1985**, *4* (1), 83–91.

(17) Kao, S. C.; Gaus, P. L.; Youngdahl, K.; Darensbourg, M. Y. Selective Reduction of Acyl Chlorides to Aldehydes by Anionic-6B Transition-Metal Hydrides. *Organometallics* **1984**, *3* (10), 1601–1603.

10.1021/om701218x CCC: $40.75
Publication on Web 05/17/2008

by the free energy for reaction 1, $\Delta G^0_{H^-}$. Thus a larger value of $\Delta G^0_{H^-}$ corresponds to a poorer hydride donor, and a smaller value corresponds to a better hydride donor.

$$[HM(diphosphine)_2]^+ \rightarrow [M(diphosphine)_2]^{2+} + H^- \quad \Delta G^0_{H^-} \tag{1}$$

The hydride donor abilities of a series of $[HM(diphosphine)_2]^+$ complexes have been measured for Ni, Pd, and Pt.[29–35] Two experimental approaches were used to obtain hydride donor abilities, $\Delta G^0_{H^-}$, which are shown in Scheme 1 and Scheme 2. In the first approach, the pK_a of $HML_2{}^{+2}$ and the potentials of $[ML_2]/[ML_2]^{2+}$ couples, E^0(II/0), were measured. $\Delta G^0_{H^-}$ was calculated from these values and the known potential of the $[H^+]/[H^-]$ couple, $E^0(H^+/H^-)$. Scheme 1 shows the corresponding reactions for these experimental thermodynamic values, eqs 2, 3, and 4, where the constants required to convert these values into free energies (kcal mol^{-1}) are also shown. The equation used to calculate $\Delta G^0_{H^-}$ is shown in reaction 5. In the second approach, the equilibrium constant for the heterolytic cleavage of hydrogen with ML^{+2} and a base, K_r, was measured as well as the pK_a of the base. These values and the known heterolytic bond energy of hydrogen, $\Delta G^0_{H2,het}$, were used to obtain $\Delta G^0_{H^-}$. Scheme 2 shows the reactions for this scheme, 6, 7, and 8, as well as the equation used to determine $\Delta G^0_{H^-}$.

Scheme 1

$HML_2^+ \rightarrow ML_2 + H^+$	$\Delta G^0 = 1.37pK_a(HML_2^+)$	(2)
$ML_2 \rightarrow ML_2^{+2} + 2e^-$	$\Delta G^0 = 46.1E^0$(II/0)	(3)
$H^+ + 2e^- \rightarrow H^-$	$\Delta G^0 = -46.1E^0(H^+/H^-)$	(4)
$HML_2^+ \rightarrow ML_2^{2+} + H^-$	$\Delta G^0_{H^-} = 1.37pKa(HML_2^+) + 46.1E^0$(II/0) + 79.6	(5)

Scheme 2

$HML_2^+ + BH^+ \rightarrow ML_2^{+2} + H_2$ (g) + B	$\Delta G^0 = 1.37pK_r$	(6)
$B + H^+ \rightarrow BH^+$	$\Delta G^0 = -1.37pK_a(BH^+)$	(7)
H_2 (g) $\rightarrow H^+$ (sol) + H^- (sol)	$\Delta G^0_{H2,het} = 76.0$	(8)
$HML_2^+ \rightarrow ML_2^{2+} + H^-$	$\Delta G^0_{H^-} = 1.37pK_r - 1.37pK_a(BH^+) + 76.0$	(9)

Table 1. Previous Experimental[a] Values for $\Delta G^0_{H^-}$ (kcal mol^{-1}) for $HML_2{}^+$

	metal, M		
ligand, L	Ni	Pd	Pt
dmpe	50.7[b] (50.8[c])		42.5[c] (42.0[c])
depe	56.0[b] (56.0[c])	43.2[e]	44.2[c]
dppe	62.7[b]		52.5[d]
dmpp	61.2[b] (60.4[c])		50.7[c] (51.0[c])
depp	67.2[c] (66.2[c])	54.7[e]	(53.8[c])
depx		61.5[e]	
depPE		66.4[e]	
EtXan		70.4[e]	76.0

[a] Values determined using Scheme 1 or Scheme 2 (in parantheses). [b] Ref 34. [c] Ref 33. [d] Ref 35. [e] Ref 23.

Molecular complexes containing diphosphine ligands with a number of transition metals were prepared, and their corresponding hydride donor abilities were measured.[23,33–35] The structures and naming conventions for the ligands that are considered for this study are shown below. Several complexes with Ni, Pd, and Pt were prepared and $\Delta G^0_{H^-}$ was measured using Schemes 1 and 2. Table 1 shows these experimentally measured values. As can be seen, in cases where both approaches were used there is good agreement.

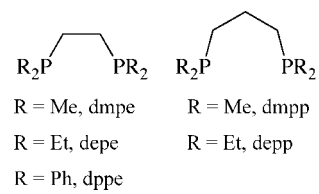

R = Me, dmpe R = Me, dmpp

R = Et, depe R = Et, depp

R = Ph, dppe

Transition metal complexes formed with these ligands are characterized by a bite angle formed by the two phosphorus atoms of each ligand and the metal center. The size of this P−M−P angle is determined by a compromise between the bite angle preferred by the metal and the bite angle preferred by the

(18) Kinney, R. J.; Jones, W. D.; Bergman, R. G. Synthesis and Reactions of (η^5-Cyclopentadienyl)tricarbonylhydridovanadate−a Comparative Mechanistic Study of Its Organic Halide Reduction Reactions with Those of Tri-Normal-Butyltin Hydride. *J. Am. Chem. Soc.* **1978**, *100* (25), 7902–7915.

(19) Martin, B. D.; Warner, K. E.; Norton, J. R. Mechanism of the Reaction of a Solvated Rhenium Acyl Complex with Neutral Transition-Metal Hydrides−Relative Nucleophilicity of Such Hydrides. *J. Am. Chem. Soc.* **1986**, *108* (1), 33–39.

(20) Hembre, R. T.; McQueen, J. S. "Redox-Switch" Catalysis of C-C Bond Formation with H^{-2}: One-Electron Reduction of the Trityl Cation. *Angew. Chem., Int. Ed. Engl.* **1997**, *36* (1−2), 65–67.

(21) Hembre, R. T.; McQueen, S. Hydrogenase Enzyme Reactivity Modeling with a Transition-Metal Dihydrogen Complex. *J. Am. Chem. Soc.* **1994**, *116* (5), 2141–2142.

(22) Cheng, T. Y.; Brunschwig, B. S.; Bullock, R. M. Hydride Transfer Reactions of Transition Metal Hydrides: Kinetic Hydricity of Metal Carbonyl Hydrides. *J. Am. Chem. Soc.* **1998**, *120* (50), 13121–13137.

(23) Raebiger, J. W.; DuBois, D. L. Thermodynamic Studies of $HRh(depx)_2$ and $[(H)_2Rh(depx)_2](CF_3SO_3)$: Relationships between Five-Coordinate Monohydrides and Six-Coordinate Dihydrides. *Organometallics* **2005**, *24* (1), 110–118.

(24) Ellis, W. W.; Raebiger, J. W.; Curtis, C. J.; Bruno, J. W.; DuBois, D. L. Hydricities of BzNADH, $C_5H_5MO(PMe_3)(CO)_2H$, and $C_5Me_5Mo(PMe_3)(CO)_2H$ in Acetonitrile. *J. Am. Chem. Soc.* **2004**, *126* (9), 2738–2743.

(25) Price, A. J.; Ciancanelli, R.; Noll, B. C.; Curtis, C. J.; DuBois, D. L.; DuBois, M. R. $HRh(dppb)_2$, a Powerful Hydride Donor. *Organometallics* **2002**, *21* (22), 4833–4839.

(26) Ciancanelli, R.; Noll, B. C.; DuBois, D. L.; DuBois, M. R. Comprehensive Thermodynamic Characterization of the Metal−Hydrogen Bond in a Series of Cobalt−Hydride Complexes. *J. Am. Chem. Soc.* **2002**, *124* (12), 2984–2992.

(27) Ellis, W. W.; Miedaner, A.; Curtis, C. J.; Gibson, D. H.; DuBois, D. L. Hydride Donor Abilities and Bond Dissociation Free Energies of Transition Metal Formyl Complexes. *J. Am. Chem. Soc.* **2002**, *124* (9), 1926–1932.

(28) Labinger, J. A. In *Transition Metal Hydrides: Recent Advances in Theory and Experiment*; Dedieu, A., Ed.; VCH: New York, 1991; pp 361−379.

(29) Miedaner, A.; Raebiger, J. W.; Curtis, C. J.; Miller, S. M.; DuBois, D. L. Thermodynamic Studies of $[HPt(EtXantphos)_2]^+$ and $[(H)_2Pt(EtXantphos)_2]^{2+}$. *Organometallics* **2004**, *23* (11), 2670–2679.

(30) Raebiger, J. W.; Miedaner, A.; Curtis, C. J.; Miller, S. M.; Anderson, O. P.; DuBois, D. L. Using Ligand Bite Angles to Control the Hydricity of Palladium Diphosphine Complexes. *J. Am. Chem. Soc.* **2004**, *126* (17), 5502–5514.

(31) Curtis, C. J.; Miedaner, A.; Ciancanelli, R.; Ellis, W. W.; Noll, B. C.; DuBois, M. R.; DuBois, D. L. $[Ni(Et_2PCH_2NMeCH_2PEt_2)_2]^{2+}$ as a Functional Model for Hydrogenases. *Inorg. Chem.* **2003**, *42* (1), 216–227.

(32) Curtis, C. J.; Miedaner, A.; Raebiger, J. W.; DuBois, D. L. Periodic Trends in Metal Hydride Donor Thermodynamics: Measurement and Comparison of the Hydride Donor Abilities of the Series $HM(PNP)_2{}^+$ (M = Ni, Pd, Pt; PNP = $Et_2PCH_2N(Me)CH_2PEt_2$). *Organometallics* **2004**, *23* (3), 511–516.

(33) Curtis, C. J.; Miedaner, A.; Ellis, W. W.; DuBois, D. L. Measurement of the Hydride Donor Abilities of $[HM(diphosphine)_2]^+$ Complexes (M = Ni, Pt) by Heterolytic Activation of Hydrogen. *J. Am. Chem. Soc.* **2002**, *124* (9), 1918–1925.

(34) Berning, D. E.; Miedaner, A.; Curtis, C. J.; Noll, B. C.; DuBois, M. C. R.; Dubois, D. L. Free-Energy Relationships between the Proton and Hydride Donor Abilities of $[HNi(diphosphine)_2]^+$ Complexes and the Half-Wave Potentials of Their Conjugate Bases. *Organometallics* **2001**, *20* (9), 1832–1839.

(35) Berning, D. E.; Noll, B. C.; DuBois, D. L. Relative Hydride, Proton, And Hydrogen Atom Transfer Abilities of $[HM(diphosphine)_2]PF_6$ Complexes (M = Pt, Ni). *J. Am. Chem. Soc.* **1999**, *121* (49), 11432–11447.

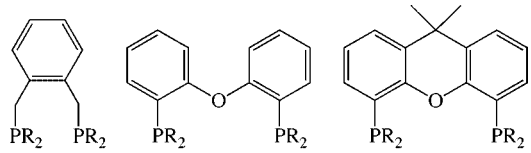

R = Me, dmpx R = Me, dmpPE R = Me, MeXan

R = Et, depx R = Et, depPE R = Et, EtXan

ligand structure (the natural bite angle).[36–38] This bite angle, β, is shown below for Ni(dmpe)$_2^{+2}$. The correlation of $\Delta G^0_{H^-}$ with β was demonstrated for several complexes through a comparison of X-ray diffraction measurements of the crystal structures and experimental measurements of $\Delta G^0_{H^-}$ of the corresponding five-coordinate [HM(diphosphine)$_2$]$^+$ complexes.[29–35] In particular, the palladium complexes with the ethyl-substituted ligands in Table 1 showed a decrease in $\Delta G^0_{H^-}$ of the hydride with a systematic decrease in β of the corresponding [M(diphosphine)$_2$]$^{2+}$ complexes determined from crystal structures. For these palladium complexes, $\Delta G^0_{H^-}$ increased following the trend depe < depp < depx < depPE < EtXan, which corresponds to an increase in β.

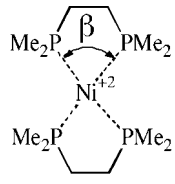

bite angle, β

The experimental studies of the hydride donor abilities also showed that $\Delta G^0_{H^-}$ depended upon a relative twist, α, of the two planes defined by the phosphorus atoms of the diphosphine ligands and the metal center as is shown below. As the bite angle is increased, steric interactions between the ligands force the ligands from a square-planar configuration for small bite angles to a more tetrahedral metal bonding for larger bite angles. It was pointed out, on the basis of extended Hückel molecular orbital calculations, that this twisting results in a more stable hydride because the LUMO of the [M(diphosphine)$_2$]$^{2+}$ complex is lowered as one proceeds from a square-planar to a tetrahedral structure. This orbital will accommodate an electron in the [M(diphosphine)$_2$]$^+$ complex, and its energy can be an indicator of the stability of the hydride.

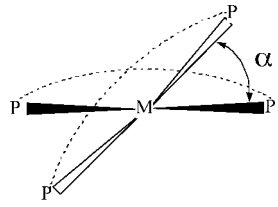

twist angle, α

In this study the hydride donor abilities of [HM(diphosphine)$_2$]$^+$ complexes (for M = Ni, Pd, and Pt) are studied using density functional theory. Of particular interest is the correlation of the hydride donor abilities with the bite angle that the phosphorus atoms make with the metal, β, and the twist angle between the two ligands, α. Free energies of metal complexes with and without a hydride are compared to extract relative hydride donor abilities from calculation in the gas phase and in a solvent (acetonitrile). A PCM (polarizable continuum model) solvent model is used, as this method has been shown to reproduce experimental results for [HM(diphosphine)$_2$]$^+$ complexes with diphosphine ligands containing ethyl and propyl bridges.[39] A similar approach has recently been used[40] in an extensive computational study of hydride donor abilities of a number of Ni and Co group metal complexes. The comparison of the calculated and experimental hydride donor abilities was outstanding. The authors further investigated a linear relationship between hydride donor ability and the natural bite angle. In this study we investigate the dependence of the hydride donor ability upon the twist angle between the ligands and show how this angle affects the lowest unoccupied molecular orbital of the [M(diphosphine)$_2$]$^{2+}$ complex, leading to changes in hydride donor ability of the corresponding [HM(diphosphine)$_2$]$^+$ complex.

Computational Details

Density functional calculations were conducted using the Gaussian03 suite of programs[41] on a Linux cluster. Molecular geometries were initially optimized using the pure functional[42,43] BLYP in the absence of solvent using the Stuttgart/Dresden effective core potential[44] (SDD) for the metal atoms and split valence basis sets for the ligands, 6-31G(d) for[45] P and 3-21G for[46] C, H, and O. Since it was seen that the algorithms employed did not scale efficiently beyond four processors on the hardware employed, and because of the numerous stable conformers possible within the systems, the size of the ligands that could be simulated were limited. For instance, we could only obtain geometries and energies for complexes with ethyl-substituted ligands with ethyl and propyl

(36) Casey, C. P.; Whiteker, G. T. The Natural Bite Angle of Chelating Diphosphines. *Isr. J. Chem.* **1990**, *30* (4), 299–304.

(37) Dierkes, P.; van Leeuwen, P. The Bite Angle Makes the Difference: A Practical Ligand Parameter for Diphosphine Ligands. *J. Chem. Soc., Dalton Trans.* **1999**, (10), 1519–1529.

(38) van Leeuwen, P.; Kamer, P. C. J.; Reek, J. N. H.; Dierkes, P. Ligand Bite Angle Effects in Metal-Catalyzed C−C Bond Formation. *Chem. Rev.* **2000**, *100* (8), 2741–2769.

(39) Kovacs, G.; Papai, I. Hydride Donor Abilities of Cationic Transition Metal Hydrides from DFT-PCM Calculations. *Organometallics* **2006**, *25* (4), 820–825.

(40) Qi, X. J.; Fu, Y.; Liu, L.; Guo, Q. X. Ab Initio Calculations of Thermodynamic Hydricities of Transition-Metal Hydrides in Acetonitrile. *Organometallics* **2007**, *26* (17), 4197–4203.

(41) Frisch, M. J.; Trucks, G. W.; Schlegel, H. B.; Scuseria, G. E.; Robb, M. A.; Cheeseman, J. R.; Montgomery, J. A.; J.; Vreven, T.; Burant, J. C.; Millam, J. M.; Iyengar, S. S.; Tomasi, J.; Barone, V.; Mennucci, B.; Cossi, M.; Scalmani, G.; Rega, N.; Petersson, G. A.; Nakatsuji, H.; Hada, M.; Ehara, M.; Toyota, K.; Fukuda, R.; Hasegawa, J.; Ishida, M.; Nakajima, T.; Honda, Y.; Kitao, O.; Nakai, H.; Klene, M.; Li, X.; Knox, J. E.; Hratchian, H. P.; Cross, J. B.; Adamo, C.; Jaramillo, J.; Gomperts, R.; Stratmann, R. E.; Yazyev, O.; Austin, A. J.; Cammi, R.; Pomelli, C.; Ochterski, J. W.; Ayala, P. Y.; Morokuma, K.; Voth, G. A.; Salvador, P.; Dannenberg, J. J.; Zakrzewski, V. G.; Dapprich, S.; Daniels, A. D.; Strain, M. C.; Farkas, O.; Malick, D. K.; Rabuck, A. D.; Raghavachari, K.; Foresman, J. B.; Ortiz, J. V.; Cui, Q.; Baboul, A. G.; Clifford, S.; Cioslowski, J.; Stefanov, B. B.; Liu, G.; Liashenko, A.; Piskorz, P.; Komaromi, I.; Martin, R. L.; Fox, D. J.; Keith, T.; Al-Laham, M. A.; Peng, C. Y.; Nanayakkara, A.; Challacombe, M.; Gill, P. M. W.; Johnson, B.; Chen, W.; Wong, M. W.; Gonzalez, C.; Pople, J. A. *Gaussian 03*; Gaussian, Inc.: Wallingford, CT, 2001.

(42) Becke, A. D. Density-Functional Exchange-Energy Approximation with Correct Asymptotic-Behavior. *Phys. Rev. A* **1988**, *38* (6), 3098–3100.

(43) Lee, C. T.; Yang, W. T.; Parr, R. G. Development of the Colle-Salvetti Correlation-Energy Formula into a Functional of the Electron-Density. *Phys. Rev. B* **1988**, *37* (2), 785–789.

(44) Fuentealba, P.; Stoll, H.; Vonszentpaly, L.; Schwerdtfeger, P.; Preuss, H. On the Reliability of Semi-Empirical Pseudopotentials−Simulation of Hartree−Fock and Dirac−Fock Results. *J. Phys. B-At. Mol. Opt. Phys.* **1983**, *16* (11), L323−L328.

(45) Ditchfie, R.; Hehre, W. J.; Pople, J. A. Self-Consistent Molecular-Orbital Methods. Extended Gaussian-Type Basis for Molecular-Orbital Studies of Organic Molecules. *J. Chem. Phys.* **1971**, *54* (2), 724&

(46) Binkley, J. S.; Pople, J. A.; Hehre, W. J. Self-Consistent Molecular-Orbital Methods. Small Split-Valence Basis-Sets for First-Row Elements. *J. Am. Chem. Soc.* **1980**, *102* (3), 939–947.

Table 2. Calculated and Experimental[a] Molecular Geometries

	BLYP in vacuum[b]			BLYP w/ PCM[c]			B3LYP[d]
complex	P−M−P_{av}	twist	P−M_{av}	$\Delta\Delta G^0_{H^-}$ eq 11, kcal mol^{-1}	twist	$\Delta\Delta G^0_{H^-}$ eq 11, kcal mol^{-1}	$\Delta\Delta G^0_{H^-}$ eq 11, kcal mol^{-1}
$Ni(dmpe)_2^{+2}$	86.1 (86.1)	7.5 (3.4)	2.28 (2.21)	0.0 (0.0)	7.3 (3.4)	0.0 (0.0)	0.0 (0.0)
$Ni(depe)_2^{+2}$	85.4 (84.8)	0.0 (0.0)	2.31 (2.24)	−7.9 (5.3)	12.6 (0.0)	2.6 (5.3)	5.5 (5.3)
$Ni(dmpp)_2^{+2}$	90.4 (92.9)	49.5 (51.5)	2.30 (2.20)	6.9 (10.5)	52.8 (51.5)	10.4 (12.3)	13.4 (12.3)
$Ni(depp)_2^{+2}$	88.6	34.5	2.32	−2.5 (16.5)	36.0	7.7 (16.5)	10.4 (16.5)
$Pd(depe)_2^{+2}$	84.2	5.4	2.42	−15.0 (−7.5)	5.5	−10.3 (−5.7)	−5.8 (−5.7)
$Pd(depp)_2^{+2}$	86.6 (86.1)	24.6 (22.3)	2.45 (2.37)	−12.8 (4.0)	24.8 (22.3)	4.9 (4.0)	7.5 (4.0)
$Pt(dmpe)_2^{+2}$	84.2	6.8	2.40	−13.3 (−8.2)	5.0	−9.1 (−10.1)	−5.7 (−10.1)
$Pt(depe)_2^{+2}$	84.0	0	2.42	−23.3 (−6.5)	4.3	−23.3 (−6.5)	−7.1 (−6.5)
$Pt(dmpp)_2^{+2}$	87.8 (88.1)	12.2 (11.5)	2.43 (2.31)	−11.7 (0.0)	11.3	−5.6 (−1.7)	−2.3 (−1.7)
$Pt(depp)_2^{+2}$	86.7	26.3	2.44	−18.2 (3.1)	30.6	5.0 (3.1)	2.7 (3.1)

[a] Crystal structures where available in parantheses ref 35 for Ni and Pt complexes, ref 30 for the Pd complex. [b] BLYP/SDD[M]+6-31G(d)[P]+3-21[H,C,O]. [c] BLYP/SDD[M]+6-31G(d)[P, C, O, H] with PCM-UA0 solvent model. [d] Single-point B3LYP/SDD[M]+6-31G(d)[P, C, O, H] with the PCM-UA0 solvent model.

bridges (i.e., depe and depp). We could not obtain optimized geometries for the other ethyl-containing ligands (depx, depPE, and EtXan) of the substituted palladium complexes shown in Table 1. Instead, we conducted simulations of the methyl-substituted analogues of these ligands in Ni, Pd, and Pt complexes.

In order to test the performance of this approach, we compared the geometries and energies of several calculated complexes with the experimental crystal structures, where available, and the measured values of $\Delta G^0_{H^-}$ for the hydride. Table 2 shows bite angles, metal phosphorus (M−P) bond lengths, and twist angles obtained for these compounds using this vacuum BLYP approach. As shown, these calculations produced a reasonable match to experimental crystal structures, with the exception of the M−P bond lengths. The calculated average bite angles have a root-mean-square error, rmse $= (\sum(\alpha_{exp} - \alpha_{calc})^2/N)^{1/2}$, of 1.2° with a maximum deviation of 2.5°. The calculated values of the M−P bond lengths are consistently 60 to 90 mÅ larger than the bond lengths measured in crystals. This effect has been observed before and could be an indication that the bonds are shortened due to crystal packing or an indication of the inaccuracy of the computational technique. Finally, the calculated twist angles are reasonably close to the experimental values with the rmse = 2.3° and the maximum error of 4.1°.

While BLYP calculations under vacuum produce molecular geometries consistent with crystal structures, the free energies obtained from these calculations do not correlate with the experimental $\Delta G^0_{H^-}$. In addition to optimizing the structure of the ML_2^{+2}, we also obtained geometries and energies for the hydrides, HML_2^{+}. Even though these calculations did not incorporate solvent effects, we determined if these calculations could reasonably reproduce experimental trends in the experimental $\Delta G^0_{H^-}$, by calculating relative values for the complexes shown in Table 2. The hydride donor ability, $\Delta G^0_{H^-}$, can be written as

$$\Delta G^0_{H^-} = G^\circ(ML_2^{+2}) + G^\circ(H^-) - G^\circ(HML_2^{+1}) \quad (10)$$

where $G^\circ(ML_2^{+2})$ and $G^\circ(HML_2^{+})$ are the free energies for the gas phase species obtained using BLYP. We determined the relative hydride donor free energy, $\Delta\Delta G^0_{H^-}$, using eq 11.

$$\Delta\Delta G^0_{H^-} = G^\circ(ML_2) - G^\circ(HML_2) - G^\circ(Ni(dmpe)_2) + G^\circ(NiH(dmpe)_2) \quad (11)$$

Here the calculated free energies in Table 2 are compared to the value obtained for the $HNi(dmpe)_2^{+}$ complex. The calculated values of $\Delta\Delta G^0_{H^-}$ are shown in Table 2 for the vacuum BLYP technique, where they are compared to the experimental hydricities measured in acetonitrile. As can be seen, the relative vacuum hydricities from the calculations do not correspond to the relative experimental hydride donor abilities measured in acetonitrile. The rmse of the relative hydricities of the vacuum calculations compared to the experimental measurements was 17.3 kcal mol^{-1}, with the highest deviation being 21.3 kcal mol^{-1}. Clearly this approach is not adequate for characterizing the relative hydride donor abilities of these compounds.

In order to obtain more accurate hydride donor abilities, calculations were made using an implicit solvation model. This study used the polarized continuum model[47] (PCM-UA0) with the acetonitrile dielectric constant, which when used with DFT produced accurate hydride donor abilities.[39] The geometries were reoptimized with BLYP in PCM-UA0 using the SDD basis set for the metal atoms and the 6-31G(d) split level basis set for all of the other atoms. There was little change in the bite angles or in the M−P bond lengths, but there were some changes in the twist angles. The twist angles and the calculated relative hydride donor abilities, $\Delta\Delta G^0_{H^-}$, as determined using eq 11, are shown in Table 2. As can be seen, the calculated twist angle for $[Ni(depe)_2]^{2+}$ changed significantly in the presence of the acetonitrile solvent. The rmse for the twist relative to the crystal twist was 6.0°, with the maximum difference being 12.6°. It is not clear how much of this difference is due to the computational technique or the fact that the experimental geometries come from crystal measurements. With PCM and the larger basis set, the rmse of the calculated $\Delta\Delta G^0_{H^-}$ values improved to 5.3 kcal mol^{-1} with a maximum deviation of 8.8 kcal mol^{-1}. While these deviations are much improved over the gas phase calculations, they are still high. In order to further improve the calculated hydride donor abilities, single-point energies were calculated using the hybrid functional[48] B3LYP with PCM-UA0 and the molecular geometries optimized at BLYP with PCM-UA0. B3LYP has been shown to produce accurate energies for hydrocarbons and for transition metal compounds. The SDD basis set was used for the metal atoms, and the 6-31G(d) basis set was used for other atoms. The calculated $\Delta\Delta G^0_{H^-}$ values from the single-point calculations are shown in Table 2. As can be seen, the match to experimental values is good and the standard deviation is 2.0 kcal mol^{-1} with a maximum deviation of 3.3 kcal mol^{-1}. This approach is used here to study trends in $\Delta G^0_{H^-}$.

Results and Discussion

Model Ligands. Initial calculations were conducted using metals and simplified ligands in order to systematically vary the bite angle of the diphosphine ligand and investigate its effect

(47) Cossi, M.; Scalmani, G.; Rega, N.; Barone, V. New Developments in the Polarizable Continuum Model for Quantum Mechanical and Classical Calculations on Molecules in Solution. *J. Chem. Phys.* **2002**, *117* (1), 43–54.

(48) Becke, A. D. Density-Functional Thermochemistry. The Role of Exact Exchange. *J. Chem. Phys.* **1993**, *98* (7), 5648–5652.

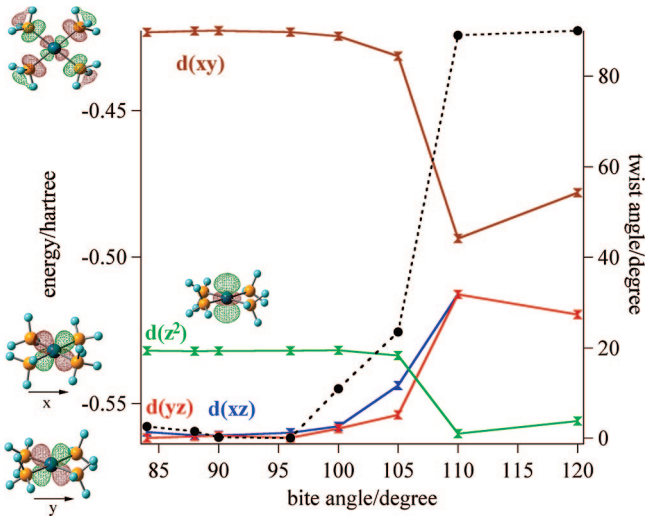

Figure 1. Plot of orbital energies and twist angle as a function of fixed bite angle between P atoms in $Pd(PH_3)_4^{+2}$ complexes.

upon twist angle and electronic structure. In these calculations the diphosphine ligands were replaced with two phosphine, PH_3, or trimethyl phosphine, $P(CH_3)_3$, ligands with a fixed P−M−P angle (see below for Pd).

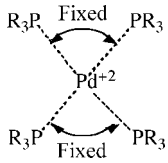

Here all of the other degrees of freedom of the molecule were allowed to vary during geometry optimization. Calculations were conducted with effective bite angles from 84° to 130° for both Pd^{2+} and Ni^{2+} metal centers. For the smallest bite angles, the complexes maintained a square-planar configuration with small twist angles, but as the bite angles increase, the molecules distorted toward a tetrahedral shape. This increase in twist angle with increasing bite angle is consistent with experimental observations of diphosphine ligands. The results for vacuum calculations (BLYP) of Pd are shown in Figures 1 and 2a for PH_3 and $P(CH_3)_3$ ligands and are similar to those obtained for Ni^{2+} under vacuum and using the PCM solvent model. The dotted lines in these figures show that as the effective bite angle increases from 80° to 110°, the molecule distorts from a twist angle of 0° (square planar) to a twist angle of 90° (tetrahedral). Similar calculations for $MH(PR_3)^+_4$ complexes, where R is H or CH_3, all produced tetrahedral structures with little change in the orbital energies as a function of bite angle. This suggests that variations in hydride donor abilities arise primarily from the molecular orbital energies of the $M(PR_3)^{+2}$ complex.

Interestingly, the plots in Figures 1 and 2a show that the preferred twist angle between pairs of ligands changes dramatically when H atoms were replaced with methyl groups. For PH_3 ligands the twist angle changes abruptly from about 0° (square planar) at a bite angle of 96° to a twist angle of 90° (tetrahedral) at a bite angle of 110°. For the $P(CH_3)_3$ ligands the change in twist angle occurs more slowly and over a larger range of bite angles. This demonstrates that the twist angle in this model system is dependent upon steric effects in the phosphine ligands and suggests that larger alkyl groups on the phosphines will increase steric interactions between ligands. This will increase

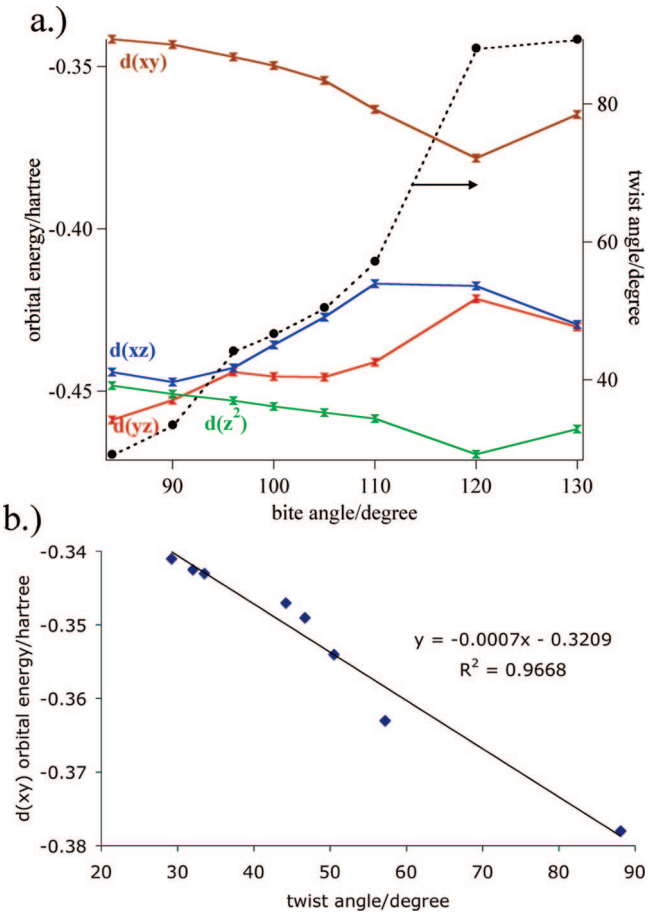

Figure 2. (a) Plot of orbital energies and twist angle as a function of fixed bite angle between P atoms in $Pd(P(CH_3)_3)_4^{+2}$ complexes. (b) Plot of the orbital energy of the d(*xy*) orbital as a function of twist angle. A linear fit to the data is shown.

the twist angle and decrease the hydride donor abilities of these complexes. This effect has been observed experimentally.

Figures 1 and 2a also contain plots of the Kohn−Sham energies of the frontier orbitals. The antibonding (M−P) LUMO has significant d(xy) character. It is this orbital that receives an electron during hydride donation, and thus an increase in the d_{xy} Kohn−Sham energy would herald a less stable hydride complex. At an effective bite angle of 84° the complex has a planar geometry with a twist angle of 0°. In this geometry, high overlap between the Pd d_{xy} orbital and lone pair orbitals of P atoms of the ligand lead to a high energy for this antibonding orbital. As the bite angle increases, there is increased steric interaction between the ligands, which eventually forces the complex to undergo a tetrahedral distortion. In the tetrahedral structure, the ligand lone pair orbitals do not overlap well with the d_{xy} orbital of Pd and the energy of the LUMO decreases. The d_{xy} orbital is occupied in the hydride complexes, and the stabilization of this orbital in the tetrahedral configuration leads to a smaller energy difference between $[HM(diphosphine)_2]^+$ and $[M(diphosphine)_2]^{+2}$ relative to the planar structure. Thus, with an increase in bite angle the $\Delta G^0_{H^-}$ decreases, and the complex becomes a poorer hydride donor. Note that for PH_3 ligands the orbital energy of d_{xy} changes abruptly between bite angles of 100° and 110°, in keeping with the abrupt change in twist angle in this range. This change in molecular orbital energies has been qualitatively shown in earlier extended Hückel

Table 3. Parameters Used to Extract $G°(H^-)$[a]

	ligand	$\Delta G^0_{H^-}$ exptl, kcal mol^{-1}	G^0 [ML_2^{+2}], hartree	G^0 [HML_2^{+2}], hartree	$\Delta G^0_{H^-}$ calc, kcal mol^{-1}
Ni	dmpe	50.7	−2012.38816	−2013.10719	50.5
	depe	56.0	−2326.64562	−2327.37341	56.0
	dmpp	61.2	−2090.93877	−2091.67918	63.9
	depp	67.2	−2405.20140	−2405.93703	60.9
Pd	depe	43.2	−2283.66166	−2284.37141	44.7
	depp	54.7	−2362.20676	−2362.93774	58.0
Pt	dmpe	42.5	−1960.88414	−1961.59412	44.8
	depe	44.2	−2275.15153	−2275.85930	43.4
	dmpp	50.7	−2091.67918	−2405.20140	48.2
	depp	53.8	−2353.74328	−2354.46662	53.2

[a] $G°(H^-) = 400.7$ kcal mol^{-1}.

Table 4. Calculated[a] and Experimental[b] Hydride Donor Abilities, Calculated Bite Angles, and Calculated Twist Angles

	Ni				Pd				Pt			
	$\Delta G^0_{H^-}$		calc	calc	$\Delta G^0_{H^-}$		calc	calc	$\Delta G^0_{H^-}$		calc	calc
	calc	expt	β	α	calc	expt	β	α	calc	expt	β	α
dmpe	50.5	50.7	86.1	7.2	45.3		84.2	4.2	44.8	42.5	84.2	8.0
depe	56.0	56.0	85.8	12.6	44.7	43.2	84.0	5.5	43.4	44.2	83.9	4.3
dmpp	63.9	60.4	91.9	52.8	55.2		86.6	23.5	48.2	50.7	87.9	11.3
depp	60.9	66.2	88.6	36.0	58.0	54.7	86.6	24.6	53.2	53.8	87.0	30.6
dmpx	68.5		94.2	54.2	61.3		89.3	32.1	62.7		90.2	36.9
dmpPE	71.3		96.2	49.5	67.7		95.6	41.1				
MeXan[c]	64.8		139.5 (97.2)	89.2 (52.2)	68.2		140.7 (97.6)	88.4 (55.8)	70.0		138.7 (97.8)	88.6 (55.6)

[a] BLYP//B3LYP with PCM-UA0 solvent model in acetonitrile. [b] Taken from Table 1. [c] The values of β and α in parentheses for the MeXan complexes are the angles P−M−P involving phosphorus atoms from different ligands and the corresponding dihedral angles. These values are used in Figures 3 and 4.

calculations[49] of the molecular orbital energies as a function of twist angle for PH_3 ligands.

The energy of the HOMOs in these model calculations can be used to predict the trend of the hydride donor abilities as a function of twist angle of diphosphine ligands. On the basis of experimental data,[30] a linear relationship exists between $\Delta G^0_{H^-}$ and the twist angle. In addition, $\Delta G^0_{H^-}$ depends linearly on the potentials of the (II/I) couples, which should correlate with the energy of the LUMO of the [M(diphosphine)$_2$]$^{2+}$ complexes. As shown in Figure 2b this orbital energy shows a linear decrease with twist angle. This linear correlation is consistent with this frontier orbital being the dominant orbital controlling the (II/I) potentials and the hydride acceptor abilities of the [M(diphosphine)$_2$]$^{2+}$ complexes.

A similar trend was observed for complexes of Ni(II). However, a notable difference between Ni and Pd is the presence of high-spin (triplet) states in tetrahedral Ni(II) complexes. For tetrahedral Ni(II) complexes the triplet states are calculated to be nearly degenerate with the singlet states, while for tetrahedral Pd(II) complexes the triplet states are more than10 kcal mol^{-1} higher. This suggests that high spin states may affect the hydride donor abilities for Ni(diphosphine)$_2$]$^{2+}$ complexes with large twist angles. Unfortunately, these nickel complexes have been difficult to synthesize. It should also be noted that calculations of the hydrides of these model complexes all had trigonal bipyramidal geometries, regardless of the bite angle. Furthermore, the energies of the metal hydride molecular orbitals were unaffected by the effective bite angles of the model complexes. Thus, it is valid to link the energies of the LUMOs of the [M(diphosphine)$_2$]$^{2+}$ complexes to the hydride donor abilities of the corresponding [HM(diphosphine)$_2$]$^+$ complexes.

Geometries and Hydride Donor Abilities for Diphosphine Complexes. Consistent with experimental observations and the calculations on the model complexes described above, calculations of hydride donor abilities of actual complexes for which the hydride donor abilities are known show that the hydride donor abilities of these complexes are dependent upon the twist angle formed by the ligands. As mentioned above, calculations using the B3LYP/SDD+6-31G(d)//BLYP/SDD+6-31G(d) model chemistry with the PCM-UA0 solvation model produced the most accurate relative $\Delta G^0_{H^-}$ values when compared to experimental values. Absolute $\Delta G^0_{H^-}$ values require a determination of the free energy of the hydride ion, $G°(H^-)$, as shown in eq 10, which is not within the scope of this study. However, an empirical value of $G°(H^-)$ can be obtained by comparison of the calculated values for [$G°(ML_2^{2+}) - G°(HML_2^+)$], to the experimental $\Delta G^0_{H^-}$. Due to size of the molecules, we were unable to obtain free energies for all of the ML_2^{2+} and HML_2^+ species in Table 1. Instead, free energies were obtained for the smallest 10 molecules in this list: Ni and Pt complexes with dmpe, depe, dmpp, and depp and Pd complexes with depe and depp. Table 3 lists the calculated and experimental values used for this determination. When the calculated free energies of all 10 complexes were used, a value of 400.7 kcal mol^{-1} was obtained for $G°(H^-)$, with an rmse of 3.2 kcal mol^{-1}. The maximum error is 6.3 kcal mol^{-1} for Ni(depp)$_2^{+2}$. The value of $G°(H^-)$ is similar to the value of 404.7 kcal mol^{-1}, using a similar approach.[39]

Using this empirical value for $G°(H^-)$ and calculated values for $G°(ML_2^{2+})$ and $G°(HML_2^+)$ the absolute $\Delta G^0_{H^-}$ values for 20 complexes with Ni, Pd, and Pt were determined, and the results, together with the calculated twist angles, are listed in Table 4. Note that $\Delta G^0_{H^-}$ was not calculated for depx, depPE, and EtXan since the size of the ligands made obtaining global minima prohibitively difficult. As can be seen, although there are no experimental values for many of the complexes in this table, these models were chosen because the results represent a wide range of bite angles, from 83° to 140°, and twist angles,

(49) Miedaner, A.; Haltiwanger, R. C.; Dubois, D. L. Relationship between the Bite Size of Diphosphine Ligands and Tetrahedral Distortions of Square-Planar Nickel(II) Complexes−Stabilization of Nickel(I) and Palladium(I) Complexes Using Diphosphine Ligands with Large Bites. *Inorg. Chem.* **1991**, *30* (3), 417–427.

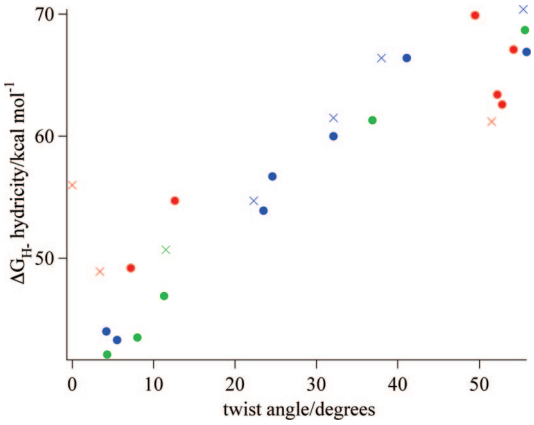

Figure 3. Plot of hydride donor abilities ($\Delta G^0_{H^-}$) versus twist angle between diphosphine ligands from Table 4. The dots are calculated using BLYP//B3LYP with pcm solvent model (see text). The ×'s are experimental hydride donor abilities plotted versus twist angles from X-ray crystal structures. The red points are for nickel complexes, the blue for palladium complexes, and the green for platinum complexes.

from 4° to 90°. For a given ligand, the bite angles are essentially the same for Pt(II) and Pd(II) complexes but increase significantly for Ni(II) complexes. This is due to a decrease in the metal phosphorus atom bond distance (Ni < Pd ≅ Pt) in these ligands. This increase in bite angle leads to a greater steric interaction between ligands, which results in a larger twist angle. As shown with the model compounds, a greater twist angle lowers the energy of the LUMO and leads to larger $\Delta G^0_{H^-}$ values. Thus, steric interactions between ligands leads to a larger twist angle and poorer hydride donor abilities.

In addition to the effects of the metal atom, there appears to be an effect due to the substituents on the diphosphine ligand. As shown in Table 1, when the sizes of the substituents are increased from dmpe to depe to dppe, the experimental values of $\Delta G^0_{H^-}$ increase. Likewise, dmpp has a lower experimental $\Delta G^0_{H^-}$ than depp. One would expect that this is due to increased steric interactions as the sizes of the substituents are increased, leading to higher twist angles, greater stabilization of the LUMO for the ML_2^{+2}, and larger $\Delta G^0_{H^-}$. For dmpe and depe ligands the calculation results follow this trend in terms of twist angle and $\Delta G^0_{H^-}$ for Ni, but for Pd and Pt the twist angle and $\Delta G^0_{H^-}$ increase with the sizes of the substituents. On the other hand, for dmpp and depp ligands the expected trend is observed for Pd and Pt, but not Ni. These twist angles are in conflict with the experimentally observed values for Ni and Pt, and it is unclear why the calculations do not correctly predict these trends. Perhaps this is due to an improper treatment of dispersion energy. Regardless of these differences, the metal size, the size of the side group, and the natural bite angle of the ligand all affect the twist angle of the complex. The accumulation of these effects can be visualized by plotting $\Delta G^0_{H^-}$ as a function of twist angle, as is done in Figure 3. As can be seen, the values appear to have a general monotonic trend with twist angle up to about 50°. The only complexes with twist angles larger than this contained MeXan ligands. The bite angles for these complexes are about 138°, larger than the angles in a tetrahedral structure (107°), and the twist angles are about 89°. As with the model compound studies, it appears as though it is difficult to form complexes with twist angles between 55° and 90°. It also appears to be difficult to form complexes with bite angles between 95° and 130°. Perhaps as the bite angle approaches 100°, the structure jumps to a tetrahedral structure, which leads to larger bite angle. In any event, the results plotted in Figure 3 and presented in Table 4 suggest that the biggest determinant for hydride donor abilities is the twist angle of the ML_2^{2+} complex, which is largely driven by steric interactions.

Table 5. Selected Molecular Parameters

	exptl[a] Et	calcd[b] Et	Me	H
		Average Bite Angle		
$Pd(dXpe)_2^{+2}$		84.2	84.2	83.3
$Pd(dXpp)_2^{+2}$	87.0	87.4	89.5	88.2
$Pd(dXpx)_2^{+2}$	90.1	89.1	89.8	93.8
$Pd(dXpPE)_2^{+2}$	94.5		95.6	93.7
$Pd(XXan)_2^{+2}$	139.7	140.1	140.7	146.35
	exptl Et	calcd Et	Me	H
		Dihedral Twist		
$Pd(dXpe)_2^{+2}$		5.4	2.4	3.0
$Pd(dXpp)_2^{+2}$	22.3	25.1	0.0	0.0
$Pd(dXpx)_2^{+2}$	32.1	34.4	36.4	0.0
$Pd(dXpPE)_2^{+2}$	38.0		41.0	19.6
$Pd(XXan)_2^{+2}$	89.0	88.4	89.1	90.0
	exptl Et	calcd Et	Me	H
		P−Pd Bond Lengths		
$Pd(dXpe)_2^{+2}$		2.42	2.41	2.39
$Pd(dXpp)_2^{+2}$	2.366	2.45	2.45	2.39
$Pd(dXpx)_2^{+2}$	2.342	2.43	2.42	2.41
$Pd(dXpPE)_2^{+2}$	2.381		2.44	2.42
$Pd(XXan)_2^{+2}$	2.338	2.43	2.40	2.37

[a] Ref 30. [b] BLYP/SDD[M]+6-31G(d)[P]+3-21[H,C,O] under vacuum.

The importance of steric interactions in determining the hydride donor abilities can be seen by comparing the calculated twist angles for Pd(II) complexes as shown in Table 5. This table compares bite angles, twist angles, and Pd−P bond lengths for complexes with hydrogen, methyl, and ethyl side groups calculated using the vacuum BLYP approach described above. Note that the size of the side group has little affect upon the bite angle but has a profound effect upon the twist angle. In particular, replacing methyl or ethyl groups with hydrogen atoms leads to the same effect seen in the model system where there is an abrupt change in twist angle as the bite angle is increased. These effects suggest that the steric interactions resulting from the side groups can increase the twist angle of the complex, which will in turn affect the hydride donor ability.

In spite of the apparent overall monotonic trend of increasing $\Delta G^0_{H^-}$ with increasing twist angle, more careful examination suggests that there is an inherent difference between Ni(II) and Pd(II) and Pt(II) complexes in addition to their effect upon the twist angle. This can be seen by fitting the $\Delta G^0_{H^-}$ vs bite angle and twist angle to a linear function, as shown in Figure 4. For the MeXan complexes, we use the P−M−P angle with phosphorus atoms from different ligands and the corresponding dihedral angles. As shown in Figure 4a, a good linear fit of $\Delta G^0_{H^-}$ vs bite angle is not obtained (r^2 = 0.77, 0.85, and 0.89 for Ni(II), Pd(II), and Pt(II) complexes). However, Figure 4b shows that a good linear fit is obtained for $\Delta G^0_{H^-}$ as a function of twist angle. For Pd(II) and Pt(II) complexes r^2 is greater than 0.94 and slopes for these two metals are similar. For Ni(II) complexes, however, the fit is not as good, and the line has a significantly different slope and intercept. This behavior suggests that there may be a more subtle electronic contribution to trends in the hydride donor abilities of Ni(II) complexes.

Conclusions

The results of these calculations show that the hydride donor abilities of the group 8 metal diphosphine complexes are primarily

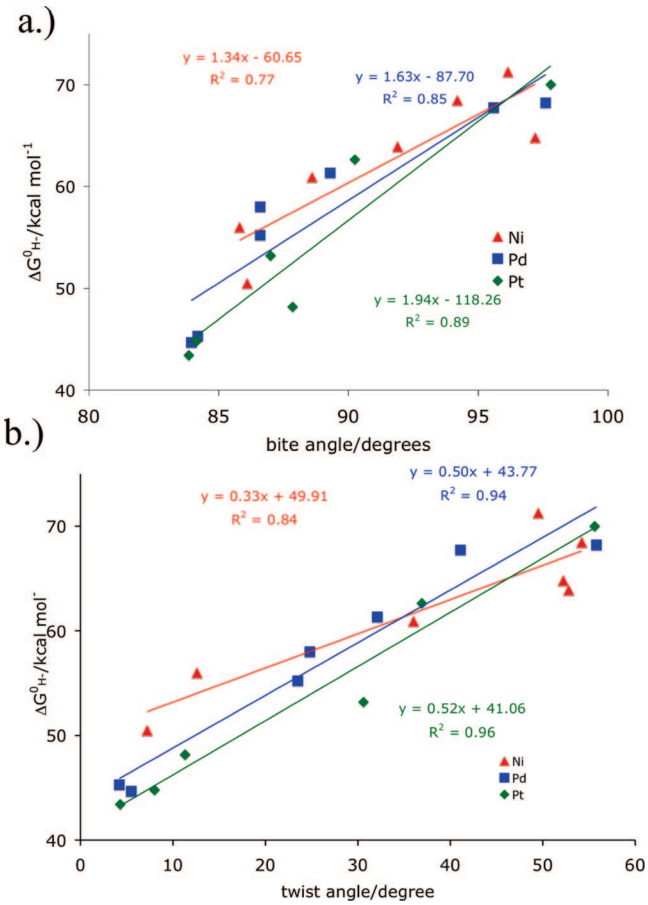

Figure 4. Plots of $\Delta G^0_{H^-}$ as a function of (a) bite angle and (b) twist angle for ML_2^{+2} for Ni^{2+} (red), Pd^{2+} (blue), and Pt^{2+} (green) from Table 4. Least-squares fits to the data are shown.

dependent upon the twist angle formed between the two ligands. In fact, there appears to be a linear relationship between this twist angle and the donor ability for bite angles up to 100°. Larger bite angles result in a tetrahedral structure with the donor ability dependent upon the dihedral angle formed by phosphorus atoms from different ligands. This relation allows one to predict the hydride donor ability if the twist angle can be determined.

The geometric parameters discussed appear to act as proxies for the more fundamental LUMO energies over limited ranges of angular coordinates. Direct plots of calculated hydricity vs d_{xy} orbital energy show satisfying correlation over all complexes studied herein. Within the limitations implied by the model chemistry used, for this class of compounds the LUMO energy alone thus appears to be the best single predictor of actual reaction hydricities. The reported results together with extant literature suggest that a full quantitative structure−activity relationship examining the predictive capabilities of bite and twist angles, orbital energies, and other calculated properties in principle may be the best means to predict reactivates of nickel group diphosphine complexes.

Acknowledgment. We would like to acknowledge useful conversations with Jeff Hay and financial support from the Laboratory Directed Research and Development Fund at the National Renewable Energy Laboratory. D.L.D. also acknowledges the support of the Office of Basic Energy Sciences of the Department of Energy, by the Chemical Sciences program. The Pacific Northwest National Laboratory is operated by Battelle for the U.S. Department of Energy.

Supporting Information Available: This material is available free of charge via the Internet at http://pubs.acs.org.

OM701218X